Selective solid phase extraction of copper using a new Cu(II)-imprinted polymer and determination by inductively coupled plasma optical emission spectroscopy (ICP-OES)

Vedat Yilmaz [a,b,*], Zikri Arslan [a,**], Orhan Hazer [c], Hayriye Yilmaz [b]

[a] Department of Chemistry and Biochemistry, Jackson State University, Jackson, USA
[b] Department of Analytical Chemistry, Faculty of Pharmacy, Erciyes University, Kayseri, Turkey
[c] Department of Chemistry, Faculty of Art and Science, Bozok University, Yozgat, Turkey

ARTICLE INFO

ABSTRACT

This work reports the preparation of a novel Cu(II)-ion imprinted polymer using 2-thiozylmethacrylamide (TMA) for on-line preconcentration of Cu(II) prior to its determination by inductively coupled optical emission spectroscopy (ICP-OES). Cu(II)-TMA monomer (complex) was synthesized and copolymerized via bulk polymerization method in the presence of ethyleneglycoldimethacrylate cross-linker. The resulting polymer was washed with 5% (v/v) HNO_3 to remove Cu(II) ions and then with water until a neutral pH. The ion imprinted polymer was characterized by FT-IR and scanning electron microscopy. The experimental conditions were optimized for on-line preconcentration of Cu(II) using a minicolumn of ion imprinted polymer (IIP). Quantitative retention was achieved between pH 5.0 and 6.0, whereas the recoveries for the non-imprinted polymer (NIP) were about 61%. The IIP showed about 30 times higher selectivity to Cu(II) in comparison to NIP. The IIP also exhibited excellent selectivity for Cu(II) against the competing transition and heavy metal ions, including Cd, Co, Cr, Fe, Mn, Ni, Pb and Zn. Computational calculations revealed that the selectivity of IIP was mediated by the stability of Cu(II)–TMA complex which was far more stable than those of Co(II), Ni(II) and Zn(II) that have similar charge and ionic radii to Cu(II). A volume of 10 mL sample solution was loaded onto the column at 4.0 mL min^{-1} by using a sequential injection system (FIALab 3200) followed by elution with 1.0 mL of 2% (v/v) HNO_3. The relative standard deviation (RSD) and limit of detection (LOD, 3 s) of the method were 3.2% and 0.4 μg L^{-1}, respectively. The method was successfully applied to determination of Cu(II) in fish otoliths (CRM 22), bone ash (SRM 1400) and coastal seawater and estuarine water samples.

© 2013 Elsevier B.V. All rights reserved.

1. Introduction

Copper (Cu) is a biologically essential element that plays important roles in metabolism, including antioxidant effects, energy generation, incorporation of Fe into hemoglobin [1–3]. It is also an important trace element in seawater for the growth of phytoplankton in the ocean [4,5]. However, excessive levels of Cu could induce oxidative stress on microorganisms and gastrointestinal distress and even liver and kidney damage on humans under long-term exposure. According to the USEPA, the maximum contaminant level goal (MCLG) for copper in drinking water is 1.3 mg L^{-1} to protect human health against exposure to excessive levels of Cu.

Inductively coupled plasma optical emission spectrometry (ICP-OES) has been an established technique in trace analysis of biological and environmental samples owing to its multi-element determination capability, wide linear range and better tolerance to the matrix effects of complex samples [6,7]. Despite these advantages, ICP-OES lacks the adequate sensitivity for measurement of very low levels Cu and many other trace elements. Determinations at sub-parts per million (sub-ppb) levels are often achieved by means of separation and preconcentration procedures to increase the elemental concentrations above the detection limits of ICP-OES while eliminating the saline matrix.

Solid phase extraction (SPE) procedures using sealed chelating columns have found wide applications because of a number of attractive features, such as ability for higher enrichment factors and reduced risk of elemental contamination [8–10]. Over the years, research in SPE evolved around the preconcentration of trace elements mainly in water samples and complex matrices using various supports containing 8-hydroxyquinoline (8-HQ) [11,12], iminodiacetate [13–15], 2,6-diacetylpyridine [16], 1-(2-thiazolylazo)-2-naphthol (TAN) [17], 1,5-bis(2-pyridyl)-3-sulphophenylmethylene thiocarbonohydrazide [18],

* Correspondence to: V. Yilmaz, Department of Analytical Chemistry, Faculty of Pharmacy, Erciyes University, Kayseri, Turkey. Tel.: +90 352 438 0486; fax: +90 352 437 9169.
** Corresponding author. Tel.: +1 601 979 2072; fax: +1 601 979 3674.
E-mail addresses: vyilmaz@erciyes.edu.tr (V. Yilmaz), zikri.arslan@jsums.edu (Z. Arslan).

nitrilotriacetate (NTA) [19], and thiacalix[4]arenetetracarboxylate [20]. Nanoscale supports, such as silica and titanium dioxide, have also been modified with chelating agents [21,22], and microorganisms [23] for solid phase extraction of trace elements from natural water samples.

Selectivity and effective removal of matrix salts are important phenomena in SPE applications. Often the chelating supports complex multiple elements unselectively and moreover retain significant levels of alkali and alkaline earth elements. Recently, molecularly imprinted polymers (MIPs) or ion-imprinted polymers (IIPs) have received popularity as highly selective sorbents for SPE [24–26]. Ion imprinting approach affords preparation of synthetic polymer receptors with enhanced selectivity for a target metal ion (e.g., template). Synthesis of an IIP is generally achieved in three steps: (1) complexation of the target metal ion (template) with appropriate ligand/s or functional monomers, (2) copolymerization of the monomers around the template using a cross-linking agent, and (3) removal of the target metal ion from the polymer yielding cavities or "imprinted sites" that are complementary in size and shape of imprint metal ion. Thus, the resultant polymer possesses improved selectivity to the template over the other ions in sample solution.

Selectivity of the IIPs increases with increasing strength of interaction between imprint ion and the ligands and functional monomers before polymerization process. Other factors, including the coordination geometry, the coordination number of the metal ion together with the charge and the size of the ion are also known to play important roles in selectivity of IIPs [27,28]. To date, different IIPs have been synthesized and applied for selective preconcentration of a number transition metal ions, including Cu(II) [29–38], Cd(II) [39,40], Ni(II) [41–43], Zn(II) [44], Pb(II) [45], Fe(III) [46], Cr(III) [47], and Hg(II) [48,49].

In this study, we utilized a new Cu(II)-imprinted polymeric support by using 2-thiozylmethacrylamide (TMA). The IIP was used as a solid phase support in a minicolumn for on-line solid phase extraction of Cu(II) from aqueous solutions and determination by ICP-OES. A series of experiments were carried out to elucidate the effects of pH and flow rate of sample solutions, acid eluent and its concentration on the analytical performance of the IIP. Selectivity of the IIP for Cu(II) was investigated in the presence of transition metal ions. Stabilization energies of Cu(II)–TMA complex and those of the competing ions (e.g., Co, Ni, and Zn) were calculated to elucidate the driving factors behind the selectivity of the polymer for Cu(II). Sorption conditions were optimized for selective extraction and preconcentration of Cu(II). The optimized method was applied to the determination of Cu(II) by ICP-OES in coastal seawater, estuarine water, bone ash and fish otolith samples.

2. Experimental

2.1. Reagents and materials

Double deionized water (DI, 18.0 MΩ cm) was used for preparation of solutions. Multielement stock solutions of Al, As, Ba, Cd, Ca, Co, Cr, Cu, Fe, Mg, Mn, Bi, Ag, Ni, Pb, Sb, Se, Sr, and Zn were prepared from a 10 μgmL^{-1} stock standard solution (SpexCertiPrep, Metuchen, NJ) in 5% (v/v) HNO$_3$ (Trace metal grade, Fisher Scientific). Ammonium acetate solution was prepared with 182 mL of trace metal grade ammonium hydroxide (NH$_4$OH, Fisher Scientific) and 112 mL of acetic acid (99.99 +%, Sigma Aldrich) in 1.0 L deionized water. The pH of the solution was adjusted to pH 9.0 with NH$_4$OH and then used for adjusting the pH of the experimental solutions to desired pH. Ethyleneglycoldimethacrylate (EGDMA), 2-Aminothiazole, and methacryloyl chloride,(Sigma Aldrich, St. Louis, MO) were used as received. 2,2-Azobisisobutyronitrile (AIBN, Acros Organics) was purified by successive crystallizations from chloroform-methanol mixture. High purity salts of the elements (e.g., Ca, Mg, Na) were used to prepare matrix solutions.

2.2. Instrumentation

A PerkinElmer (Shelton, CT, USA) Optima 3300 DV ICP-OES instrument was used for determinations. The instrument is optimized for sensitivity with 1.0 μg mL^{-1} Mn solution as needed. Measurements were made in axial view mode using the recommended wavelengths. Data collection was made by ICP-WinLab software package (version 3.1). The operation conditions for the instrument are summarized in Table 1. The pH of the solutions was adjusted by using an Oakton digital pH meter with glass electrode (Model 510).

The NMR (^{1}H) spectrum of the monomer was recorded by a BrukerAvance III 400 MHz NMR spectrometer (Karlsruhe, Germany) using dimethylsulfoxide (DMSO) as solvent and tetramethylsilane as internal standard. Infrared spectra of the monomer, monomer-Cu complex, imprinted and non-imprinted polymers were recorded using a PerkinElmer Spectrum 400 FT-IR spectrometer (Waltham, MA, USA). Elemental analysis of the monomer–Cu complex was performed by a Leco CHNSO-932 auto microanalyser (USA). The surface morphology of the polymers was examined using Leo model 440 scanning electron microscope (SEM, England).

2.3. Synthesis of Cu(II)-imprinted polymer

2.3.1. Preparation of monomer and complexation with Cu(II)

2-Thiozylmethacrylamide monomer (TMA) was synthesized as described previously [38]. Briefly, ice cold solution of 0.01 mol of methacryloyl chloride in 10 mL dichloromethane was added dropwise under stirring to 30 mL ice cold (0–5 °C) solution of dichloromethane containing 0.01 mol of 2-aminothiazole and 0.03 mol of triethylamine. The mixture was stirred for 12 h at room temperature, then filtered and evaporated with a rotavapor. The yellow product was recrystallized from ethanol with a yield of 52%.The product was characterized by proton NMR (^{1}H NMR) and FT-IR spectroscopy. The NMR spectra recorded in DMSO showed the following peaks (δ in ppm) at 2.1 (3H, CH$_3$), 5.6 (1H, CH$_2$), 5.9 (1H, CH$_2$), 7.0 (1H, CH), 7.4 (1H, CH) and 12.0 (1H, NH). The FT-IR spectra exhibited peaks at 3139 cm^{-1}(N−H amide), 3000–3100 cm^{-1} (C−H aromatic), 2925 and 2855 cm^{-1} (C−H aliphatic), 1671 cm^{-1} (C=O amide), 1629 cm^{-1} (CH$_2$=C−), 1545, 1492, 1445 cm^{-1} (C=C aromatic), 1166 cm^{-1} (C−O−C).

The monomer (TMA) was then reacted at room temperature with Cu(II) to synthesize Cu(II)–TMA complex. Specifically, 0.729 g of TMA (4 mmol,) was dissolved in 20 mL ethanol. Under stirring, and 0.379 g of CuCl$_2$.2H$_2$O (2.1 mmol) was added to this solution. The contents were reacted until the color turned to green (~6 h). The solvent was removed and the Cu(II)–TMA complex (green solid) was washed with a mixture of ethanol and acetonitrile and then dried at 60 °C. The yield was 58% (0.546 g). Chemical composition of the complex was determined to be C$_{14}$H$_{16}$N$_4$O$_2$S$_2$CuCl$_2$ by elemental analysis. The percent composition of the complex was 35.7% C, 3.42% H; 11.9% N; 13.6% S; 13.5% Cu. Experimentally determined values were 35.5% C, 3.67% H, 11.4% N, 12.9% S, and 13.8% Cu. FT-IR spectrum showed peaks at 3264 cm^{-1} (N−H amide), 3000–3100 cm^{-1} (C−H aromatic), 2925 and 2853 cm^{-1} (C−H

Table 1
Operating conditions for Optima 3300 DV ICP-OES instrument.

RF power/kW	1.5
Nebulizer	Cross-flow
Spray chamber	Concentric glass
Plasma Ar/L min^{-1}	16
Auxiliary Ar/L min^{-1}	0.4
Nebulizer Ar/L min^{-1}	0.6
Sample uptake/mL min^{-1}	1.5
Delay time (s)	45
Scanning mode	Continuous, axial
Integration time (s)	Automatic (min. 0.5–max. 5 s)
Readings/replicate	3
Wavelength (nm)	Cu, 324.754

aliphatic), 1687 cm^{-1} (C=O amide), 1629 cm^{-1} (CH$_2$=C–). Copper(II) coordinated to the monomer through the nitrogen of the thiazole ring and carbonyl oxygen as shown in Fig. 1.

2.3.2. Preparation of Cu(II)-imprinted and non-imprinted polymers

The Cu(II)-imprinted and non-imprinted polymers were prepared by bulk polymerization method. The steps involving the preparation of the Cu(II)-IIP and the processes of the sorption and desorption of the Cu(II) ions are depicted in Fig. 1. First, 0.471 g of Cu(II)–TMA complex (1 mmol) was dissolved in 10 mL of DMSO. Then, 2.3 mL of EGDMA (12 mmol) cross-linking agent and 25 mg of AIBN (0.15 mmol, free-radical initiator) were added under stirring. The solution was purged thoroughly with N$_2$ for 5 min. The reaction vial was sealed and the mixture was kept at 70 °C for 12 h. The polymerization was completed within 3 h by raising the temperature to 80 °C. The resulting green material was transferred to another vial, washed with water and dried at 60 °C for 24 h. The blocks of the polymer were ground and passed through 90–180 μm apertures (see Fig. 1S-a). The polymer was washed with 5% (v/v) HNO$_3$ for several times to remove Cu(II) and then with copious amount of water. This process yielded pale yellow polymer (Cu(II)-IIP) which was dried at 60 °C (see Fig. 1S-b). The non-imprinted polymer (e.g., NIP) was prepared similarly by using TMA, EGDMA, and AIBN without adding any Cu(II) salt (see Fig, 1S-c) and used to determine the effect of imprinting on selectivity.

2.4. Solid phase preconcentration system

SPE columns were made from 2 cm long teflon tubing (0.4 cm i.d.) which were packed with 80 mg of imprinted and non-imprinted polymers. Both ends of the columns were closed with glass wool to retain the packing material. For cleaning, each column was washed with 5% (v/v) HNO$_3$ and DI water, respectively. A FIAlab-3200 (FIAlab Instruments Inc., Bellevue, WA) sequential injection unit was used for automated solid phase preconcentration (Fig. 2). The unit is equipped with a constant-speed peristaltic pump (PP), two 30,000-step syringe pumps (SP) (Cavro, Sunnyvale, USA) with a capacity of 5 mL for sample (SP$_1$) and 1 mL for eluent (SP$_2$). An 8-port two position flow injection valve (FIV, FIAlab) was used for sample loading onto and elution from the column. The system was controlled by the FIAlab software package (version 5.0) running on personal computer.

The operation of the FIALab 3200 unit is summarized in Table 2. In stage 1, SP$_1$ aspirated 0.5 mL of sample solution at 6 mL min^{-1} and delivered to waste through port 8. In stage 2, the injection valve (IV) is switched to load position and SP$_1$ aspirated 5.0 mL of sample solution at 6 mL min^{-1} (V$_1$ at position 1). In the meantime, PP pumped dilute buffer solution (pH 5.5) through column at 6 mL min^{-1} to condition the column. Then, SP$_1$ loaded the sample solution onto the column at 4 mL min^{-1} (Stage 3). Following this step, SP$_1$ aspirated another 5 mL of sample solution and loaded onto the column. In last part of stage 3, SP$_1$ aspirated 3 mL of buffer solution (pH 5.5) and passed through to the column to deliver the remaining sample solution in the line as well as to wash the column. In stage 4, injection valve switched to

injection position for elution. SP$_2$ aspirated 1.0 mL of 2% (v/v) HNO$_3$ (V$_2$ at port 1) and then pumped through the column at 2 mL min^{-1} back-flushing the analytes into acid cleaned centrifuge vials (V$_2$ at port 3). Finally, SP$_2$ aspirated 1.0 mL of DI water (V$_2$ at port 2) and then pumped through the column. This step delivered all the acid eluent in the lines to the collection tube as well as afforded a rinsing of the column immediately after treating with the acid eluent. A total of 10 mL sample solution was preconcentrated to a final volume of 2 mL in about 1% (v/v) HNO$_3$.

2.5. Optimization of SPE conditions

The pH of the sample solutions was varied from pH 2 to 8 for 20 μg L^{-1} Cu(II) solutions (as multielement) to determine the retention of Cu(II) on the columns packed with the resins of IIP and NIP. A volume of 5 mL solution with appropriate pH was loaded onto the column at 2.0 mL min^{-1} and eluted with 1.0 mL of 5% (v/v) HNO$_3$ and then 1.0 mL of water as mentioned above. For optimization of elution conditions, the concentration of HNO$_3$ solution was varied from 0.5 to 5% (v/v), and then its volume was examined between 0.5 and 2 mL for the optimum concentration. The effect of flow rate was examined at the optimum pH for 20 μg L^{-1} multielement solution by increasing the flow rates of sample solution and acid eluent from 1.0 to 6 mL min^{-1}.

The analytical merits of the resin, including percent recovery, distribution ratio, selectivity coefficient for Cu(II) and the relative selectivity coefficient were determined under the dynamic flow system for preconcentration of 50 μg L^{-1} multielement solutions. Sorption capacities were determined by batch method in that 50 mg of IIP or NIP were equilibrated in a volume of 20 mL of 25 μg mL^{-1} Cu(II) at the optimum pH for 2 h. The concentration of Cu(II) remained in the solution was measured by ICP–OES to calculate the sorption capacity of the resin.

2.6. Sample preparation

The accuracy of the procedure was verified by determination of Cu in certified reference materials of fish otolith (CRM No. 22) and bone ash (SRM 1400). The procedure was then applied to the determination of Cu from coastal seawater and estuarine water samples. Fish otolith certified reference material (CRM No. 22) was purchased from the National Institute of Environmental Studies (NIES), Japan. Otolith samples were prepared according to the procedure described elsewhere [50]. Briefly, 50 mg sub-samples were digested in teflon tubes (4 mL) in concentrated HNO$_3$ by using a 20-well digestion block (DigiPrep Cube, SCP Science, Champlain, NY). Each sample was first wetted with water and then dissolved slowly with dilute HNO$_3$ to avoid bubbling. To completely destroy the organics, additional 1.0 mL HNO$_3$ was added and the contents were heated to dryness at 120 °C. At dryness, 1 mL water was added and reheated to dryness. At the end, the residue was dissolved with pH 5.5 buffer solution and diluted to 6 mL in 15-mL acid cleaned-test tubes.
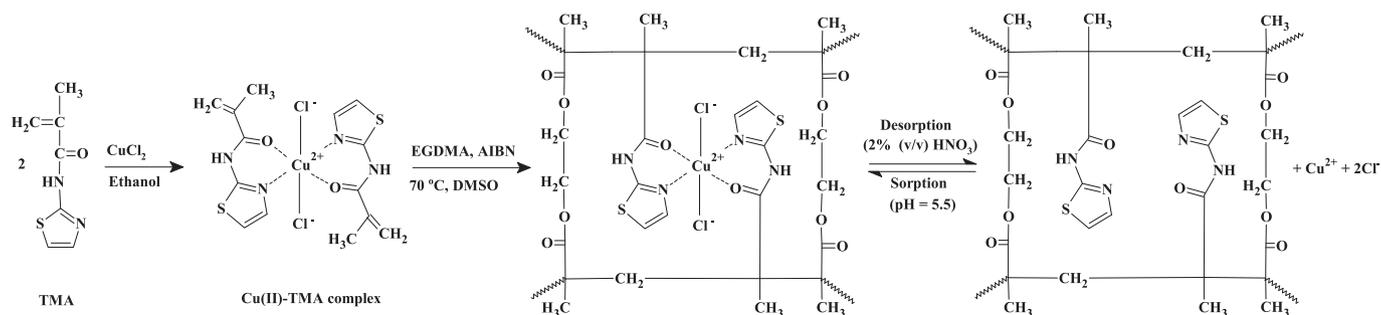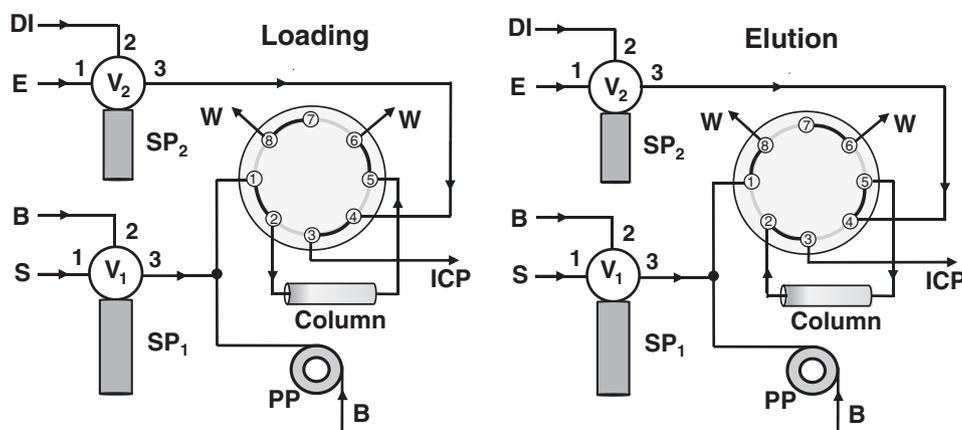

Fig. 1. Schematic representation of the synthesis of Cu(II)-TMA complex, Cu(II)-IIP and associated sorption and desorption of the Cu(II) ions.

Fig. 2. Schematic diagram of solid phase preconcentration system utilized with FIA 3200 unit and flow injection valve. SP_1 and SP_2 = Syringe pumps; PP = peristaltic pump; V_1 and V_2 = Three-way valve; S = Sample; B = Buffer (pH 5.5); E = Eluent (2% v/v HNO_3); W = Waste. The column is a teflon tubing (20 mmlong × 4 mmi.d.) packed with the Cu(II)-IIP.

Bone ash (SRM 1400) was obtained from the National Institutes of Standards and Technology, Gaithersburg, MD. It is purely calcium phosphate produced from calcinations of bone. About 50 mg sub-samples of bone ash were digested similar in concentrated HNO_3. After drying, the residue dissolved in 1.0 mL of 0.1% (v/v) HNO_3. The pH was adjusted to pH 5.5 with ammonium acetate solution (pH 9.0) and then completed to 10 mL with pH 5.5 buffer solution.

Coastal seawater was collected from Galveston Bay, Galveston, TX. Estuarine water samples were collected from the Grand Bay Estuarine Research Reserve (NERR) in the northern Gulf of Mexico along the coast of Mississippi. The water samples were placed into acid-cleaned polypropylene bottles and acidified to 0.1% (v/v) HNO_3 at the sampling site. At the laboratory, they were filtered through 0.45-μm membrane filters and stored in 0.1% v/v HNO_3 until analysis. The pH of the sub-samples was adjusted to pH 5.5 with the ammonium acetate solution and preconcentrated as for the otolith and bone ash samples.

3. Results and discussion

3.1. Characterization of Cu(II)-IIP

The IIP was characterized by Fourier transform infrared (FT-IR) spectroscopy and scanning electron microscopy (SEM). The FT-IR spectra (Fig. 3) exhibited two low intensity peaks at about 2955 and 2994 cm^{-1} associated with C–H stretching of –CH_2– and –CH_3 groups in the polymeric chain, respectively. The intense absorption centered at 1729 cm^{-1} was assigned to the carbonyl groups from EGDMA. The C–O vibration was observed at 1158 cm^{-1}. The absorption at

1637 cm^{-1} is associated to C=C and C=N (ring) stretching, while the peak at 1454 cm^{-1} was due to the –CH_2– and –CH_3 deformation.

SEM micrographs illustrating the morphologies of the IIP and NIP are shown in Fig. 4. The particles of NIP did not have a definite shape, nor did those of IIP. As expected, this structural variation was due to bulk polymerization method. The textural characteristics were closely examined at 20,000× magnification. Both polymers possessed relatively rough surfaces, which is an important factor facilitating the mass transfer rate of metal ions toward the polymer surface and consequently improving its sorption capacity. Interestingly, SEM images also indicated highly porous surfaces for NIP in comparison to IIP. Nevertheless, the NIP surfaces lacked the compatible porosity for sorption of Cu(II) as suggested the analytical results presented below. Conversely, the porous surfaces of the acid-leached IIP (e.g., Cu(II) free) revealed that the resin possessed sites or imprint pores selective for sorption of Cu(II) selectively from solution.

3.2. Optimization of Cu(II)-IIP-SPE from aqueous solutions

3.2.1. Effect of pH

TMA is immobilized on the skeleton of both NIP and IIP. Therefore, the formation of a complex between Cu(II) and TMA and hence the sorption of Cu(II) from aqueous solution is expected to be influenced by the pH of solution. The effect of pH on the sorption of Cu(II) in multielement standard solution (20 μg L^{-1}) is illustrated in Fig. 5 across a

Table 2
Operation program of the FIA 3200 unit with flow injectionvalve (FIV) during solid phase extraction.

| Stage	SP1 & SP₂ operations	V_1	V_2	FIV	
1	SP_1 aspirated 0.5 mL sample & dispensed; SP_2 = Off	1 to 3	–	Inject	Off	Line fill
2	SP_1 aspirated 5 mL sample; SP_2 = Off	1	–	Load	On	Column wash/ Sample uptake
3	SP_1 dispensed 5 mL sample; SP_2 = Off	3	–	Load	Off	Sample load
	SP_1 aspirated 5 mL sample & dispensed; SP_2 = Off	1 to 3	–	Load	Off	Sample load
	SP_1 aspirated 3 mL buffer & dispensed;SP_2 = Off	2 to 3	–	Load	Off	Column wash
4	SP_2 aspirated 1 mL eluent and dispensed; SP_1 = Off	–	1 to 3	Inject	Off	Acid Elution
	SP_2 aspirated 1 mL water & dispensed; SP_1 = Off	–	2 to 3	Inject	Off	DI elution
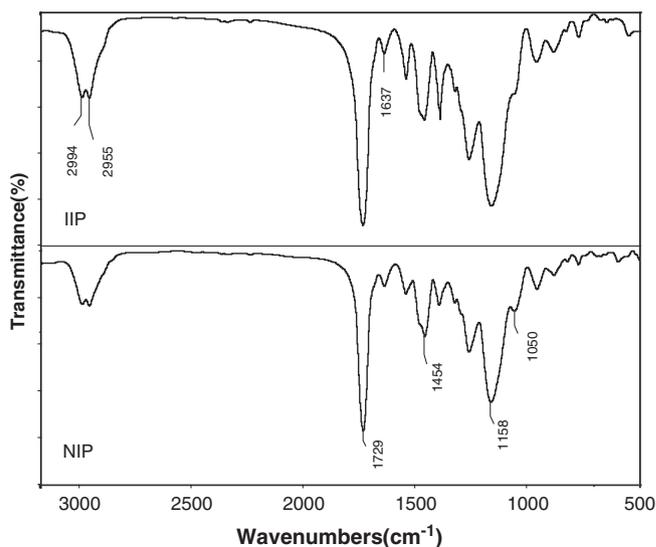
Fig. 3. FT-IR spectra of imprinted (IIP) and non-imprinted (NIP) resins.
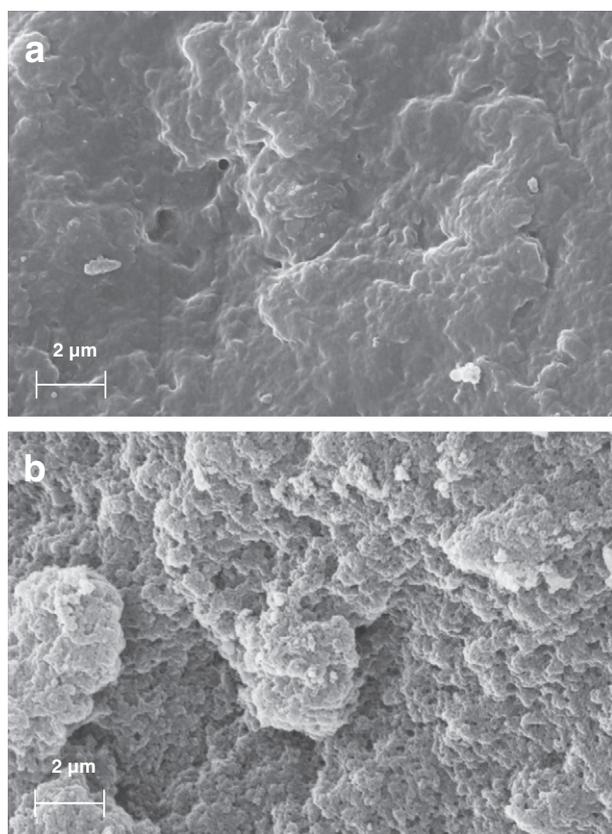
Fig. 4. Scanning electron microscope (SEM) images of (a) IIP and (b) NIP at 20,000× magnification.

pH gradient of pH 2 to 8. Maximum recovery in DI water conditions was 61% for NIP at pH 4. This result also supported the explanation above that the surfaces of NIP were not complimentary for the formation of Cu(II)-TMA despite a highly porous structure. The retention of Cu(II) on the IIP took place within a range from pH 4 to pH 6 where recoveries ranged from 91% (pH 4) to 99% (pH 5.5). In artificial seawater medium, recoveries decreased to 77% at pH 4, whereas the sorption was quantitative within pH 5 and 6 (Fig. 5). These results demonstrated that the IIP possessed strong affinity to Cu(II) even in saline solutions. A pH of 5.5 was optimum to achieve selective separation and preconcentration, therefore, subsequent studies with IIP were carried out at pH 5.5.
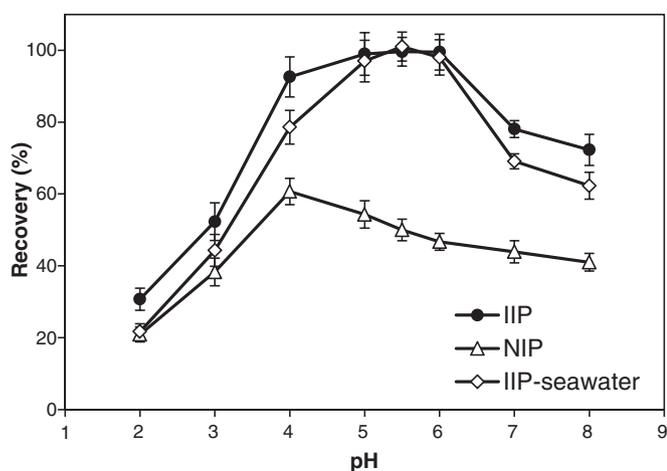
Fig. 5. The effect of solution pH on the retention of Cu(II) on the columns of IIP and NIP.

3.2.2. Optimization of elution and flow rates

Elution was examined from 0.5 to 5% (v/v) HNO_3 solutions throughout since preliminary studies proved dilute solutions of HNO_3 would be sufficient for successful removal of retained Cu(II) from the column. About 82% of Cu(II) was recovered when elution was performed with 1 mL of 0.5% (v/v) HNO_3. The recoveries were improved to 96% for 1.0 mL of 1.0% (v/v) HNO_3 indicating that a minimum of 1% (v/v) HNO_3 was required for stripping off Cu(II) from the column quantitatively. A solution of 2% (v/v) HNO_3 was chosen as the optimum eluent. Elution with different volumes (e.g., 0.5 to 2 mL) of 2% (v/v) HNO_3 showed that a volume of 1.0 mL was adequate to ensure effective cleaning of the column.

The flow rate of the sample solution influences the interaction of Cu(II) in solution with the imprinted sites on the column, and hence is an important parameter of on-line SPE procedures. No significant differences were observed in sorption efficiency when the flow rate for 20 μg L^{-1} multielement solution at pH 5.5 was examined between 1 to 6 mL min^{-1}. The recoveries for Cu(II) varied from 97% to 102%. Nonetheless, back-pressure on syringe was notable at flow rates above 5 mL min^{-1}, and hence solutions were loaded on the column at 4.0 mL min^{-1}. For elution with 2% (v/v) HNO_3, a flow rate of 2.0 mL min^{-1} was found optimum for quantitative removal of Cu(II) ions from the column.

3.2.3. Matrix effects and selectivity study

Studies concerning the artificial seawater (see Fig. 5) showed that matrix ions in seawater did not have deleterious effects on the sorption of Cu(II). The effects of common matrix ions, including Na^+, K^+, Ca^{2+}, Mg^{2+}, SO_4^{2-} and PO_4^{3-} were examined further in a series of experiments individually. The recoveries for Cu(II) are summarized in Table 3 that indicated that the IIP was unaffected from the matrix ions in seawater and saline samples.

Table 4 summarizes percent recoveries (%R), distribution ratios (K_d), selectivity coefficients (k) and relative selectivity coefficients (k') for IIP and NIP. The values were calculated using the equations: $K_d = [(C_i - C_f) / C_f] \times [\text{volume of solution (mL)}]/[\text{mass of resin (g)}]$; $k = K_d(Cu) / K_d(M)$; $k' = k_{(IIP)} / k_{(NIP)}$, where C_i and C_f are the initial and final concentrations of the metal ion in solution, respectively, and M represents the competing trace metal ion. A comparison of distribution ratios (K_d) of IIP and NIP for Cu(II) shows that Cu(II)-imprinting enhanced the selectivity to Cu(II) by a factor of about 30. It is also evident that the selectivity coefficients for NIP (k_{NIP}) are about unity or less than unity for Cd, Co, Cr, Fe, Mn, Ni, Pb and Zn. In other words, the NIP had no selectivity for Cu(II) over these metal ions, nor afforded adequate recoveries. The recovery for Cu(II) increased significantly in the IIP while those for the competing elements decreased further (see %R for IIP). This result demonstrated that polymerization in the presence of Cu(II)-TMA complex rendered Cu(II)-imprinted sites on the resulting polymer. The selectivity of IIP (k_{IIP}) improved by a factor of 390, 348, 71.7, 83.6, 795, 95.3, 121 and 78.2 over Cd, Co, Cr, Fe, Mn, Ni, Pb and Zn, respectively. The IIP also appeared to possess improved selectivity over the other competing ions, including Ag, Al, As, Bi, Se and V as indicated by higher $k_{(IIP)}$ values. Unlike the scenario above, however, the retention of these elements (e.g., recoveries) on the IIP increased slightly in comparison to that on NIP. Hence, the selectivity was due to

Table 3
The effect of foreign ions on the retention of 20 μg L^{-1} Cu(II). Values are average ± standard deviation for replicate samples (n = 3).

| Interfering ion	Added as	Concentration (mg L^{-1})	Recovery (%)
Na^+	NaCl	10,000	98 ± 4
K^+	KCl	1000	99 ± 5
Ca^{2+}	$Ca(NO_3)_2.4H_2O$	1000	103 ± 5
Mg^{2+}	$Mg(NO_3)_2.4H_2O$	1000	96 ± 4
SO_4^{2-}	Na_2SO_4	1000	97 ± 2
PO_4^{3-}	Na_3PO_4	1000	99 ± 5

Table 4
Percent recovery (%R), distribution ratios (K_d, mg L^{-1}), selectivity coefficients (k) and relative selectivity coefficients (k') for IIP and NIP.

Element	IIP			NIP			k'
	R (%)	K_d	$k_{(IIP)}$	R (%)	K_d	$k_{(NIP)}$	
Cu	96.8	1915	–	48.7	64.3	–	–
Ag	25.9	21.8	87.8	10.5	5.60	11.5	7.65
Al	62.2	102	18.8	59.0	98.9	0.65	28.9
As	41.2	43.7	43.8	46.2	54.1	1.19	36.9
Bi	58.6	88.5	21.6	52.2	66.9	0.96	22.5
Cd	7.3	4.91	390	50.5	63.7	1.01	386
Co	8.1	5.50	348	47.3	56.1	1.15	304
Cr	30.0	26.7	71.7	53.1	74.1	0.87	82.7
Fe	26.8	22.9	83.6	64.5	96.4	0.67	125
Mn	3.7	2.41	795	45.4	52.0	1.24	643
Ni	24.3	20.1	95.3	50.1	62.9	1.02	93.2
Pb	20.2	15.8	121	59.5	102	0.63	192
Se	12.9	9.31	206	8.4	5.70	11.3	18.2
V	44.9	50.9	37.6	36.0	36.2	1.78	21.2
Zn	28.2	24.5	78.2	51.1	65.3	0.98	79.4

increasing retention of Cu(II). In other words, the affinity of the resin to Ag, Al, As, Bi, Se and V did not change in IIP, which in due course suggests these elements do not compete with Cu(II)-imprinted sites on the IIP and their retention is due to the weak interactions at different sites on the resin.

3.3. Theoretical calculations

In order to elucidate the deriving phenomenon on the selectivity of IIP, computational studies were performed for Cu(II) and competitor ions, including Co(II), Ni(II) and Zn(II) that possess same charge and similar ionic radius (Cu(II) = 71 pm, Co(II) = 72 pm, Ni(II) = 69 pm and Zn(II) = 74 pm) to Cu(II) [51]. Calculations were performed with Spartan'10 and Gaussian G09 programs. A formal charge of +2 was assigned to the transition metal ions in their TMA complexes structures. The molecular models were optimized with Merck Molecular Force Field (MMFF). For constructing M(II)–TMA complexes, the coordination to the metal ion was drawn using the Spartan' 10 followed by the optimization of the geometry with MMFF. The representative molecular model of Cu(II)–TMA complex (ML2) is shown in Fig. 6 where Cu(II) coordinated to the monomer (TMA) through the nitrogen of thiazole ring and carbonyl oxygen. Total energies of M(II)-TMA complexes were calculated from the MMFF optimized geometries and were −1254.78, 772.55, 730.64 and 713.35 kJ mole^{-1} for Cu(II)–TMA, Ni(II)–TMA, Co(II)–TMA and Zn(II)–TMA, respectively. The calculated MMFF electrostatic charges of the corresponding transition metal ion complexes
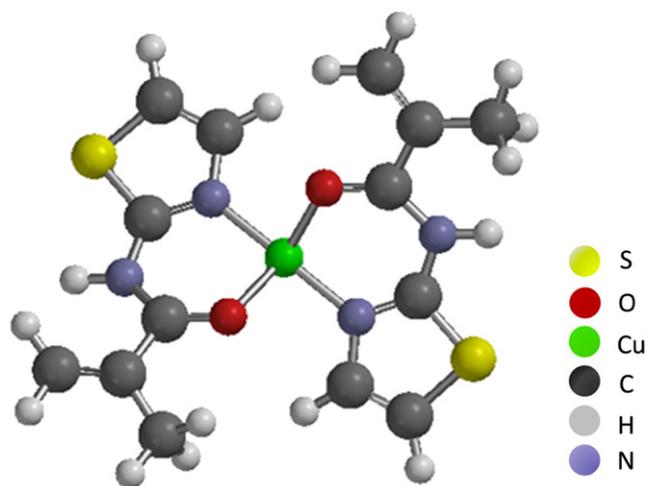
Fig. 6. Optimized molecular geometry of Cu(II)–TMA complex.

were 0.273, 0.553, 0.578 and 0.598 °C mole^{-1}, respectively. The molecular mechanics calculations revealed that there is a positive correlation between the total energy of the metal-ligand and the electrostatic charge.

Density functional theory (DFT) calculations were performed to compare the predicted stabilization energies among the selected M(II)-TMA complexes. Calculations were made using B3LYP/LANL2DZ(for metals) basis set with Gaussian G09 package. To characterize the complexes, the binding energy (ΔE_{BE}) was calculated using the equation, $\Delta E_{BE} = E_{ML} - (E_M + 2E_L)$, according to the reaction of $M(II) + 2L \rightarrow ML_2$ between the metal ion and ligand. The E_{ML}, E_M and E_L denote the energies of the complex, free metal ion, and the ligand, respectively. The geometry with minimum energy was used for the metal-ligand complex calculations. The results are summarized in Table 5 that shows that Cu(II)–TMA complex is far more stable than those of Ni(II), Co(II) and Zn(II). The data support the experimental findings confirming that the selectivity of the Cu(II)-IIP is due to the stability of Cu(II)-TMA complex. Additionally, theoretical calculations imply that successful synthesis of viable ion-imprinted polymer depends on the stability the particular metal–ligand complex as it plays a key role in rendering physical and chemical selectivity or specificity toward the metal ion in the IIP's backbone.

3.4. Sorption capacity and column stability

The sorption capacities of the IIP and NIP were determined by batch method in that 50 mg of each resin was equilibrated in 20 mL of 25 μg mL^{-1} of Cu(II) solution at pH 5.5. The solutions were gently oscillated on a shaker for 2 h. The Cu(II) concentration in determination of sorption was about three orders of magnitude higher than the levels used for method optimization. At such high levels, the retention of Cu(II) would likely be less efficient in dynamic flow system, which may result in incorrectly low capacity values for IIP. Therefore, we opted for the batch method which would provide more accurate estimate of the sorption capacity of the resin for Cu(II) owing to the extended interaction of the Cu(II) with complexing sites on the IIP. The concentration of Cu(II) remained in the solution after batch method complexation was determined by ICP–OES. The sorption capacities of the IIP and NIP for Cu(II) were found to be 76.3 and 39.3 μmol g^{-1}, respectively. This result is also consistent with the recoveries obtained under continuous flow experiments (see Table 4) where Cu(II) recoveries for IIP were about two-fold higher than that of NIP. It should be noted here that the retention of Cu(II) on the NIP is due to weak interactions, and therefore, the capacity of the NIP is expected to be much lower under salt matrix.

The performance characteristics of various ion imprinted sorbents reported for Cu(II) are summarized in Table 6. It is evident that the sorption capacity of the IIP is comparable to the capacities of the other ion imprinted materials and is sufficiently large for enrichment of trace levels of Cu(II) from complex samples. Further, the sorption capacity of the IIP is almost the same with that incorporating a Cu(II)–MTMA complex [38]. However, the results indicate that imprinted polymer of

Table 5
Predicted binding energy (ΔE_{BE}) and total energies of components for the selected metal-ligand complexes (ML$_2$) in gas phase. ($E_{TMA} = -467.40$ a.u.; 1 a.u. = 2625.5 kJ mole^{-1}; Mulliken's atomic charge of the indicated atom).

M(II)–ligand	E_M	E_{ML}	ΔE	ΔE	Mulliken
	(a.u.)	(a.u.)	(a.u)	(kJ mole^{-1})	charge
Cu(II)–TMA	−195.06	−1158.07	−28.21	−74,065	0.009
Ni(II)–TMA	−64.62	−1101.46	1.13	2,964	0.627
Co(II)–TMA	−143.06	−1077.71	1.51	3,964	0.616
Zn(II)–TMA	−168.16	−997.77	1.66	4,358	1.145

Table 6
Comparison of the sorbent characteristics of different Cu(II)-imprinted polymers.

Ligand	Method of Polymerization	Technique	Relative selectivity coefficient			Sorption capacity ($\mu mol\ g^{-1}$)	LOD ($\mu g\ L^{-1}$)	Ref. #
			$k'_{Co(II)}$	$k'_{Ni(II)}$	$k'_{Zn(II)}$			
Chitosan-succinate	Sol–gel	FAAS	16.5	122.1	5.8	750	0.83	[29]
VP/DBDA15C4[a]	Bulk	ICP-OES	13.9	11.3	16.1	75	0.5	[30]
Metacrylic acid/4-(2-pyridylazo)resorcinol	Dispersion	FAAS	19.3	16.9	nr	37	0.1	[32]
(2Z)-N,N'-bis(2aminoethylic)but-2-enediamide	Bulk	ICP-OES	64.4	208.3	49.7	469	0.32	[34]
1-Hydroxy-4(prop-2'-enyloxy)-9,10-anthraquinone	Precipitation	ICP-OES	18.1	18.7	19.4	74	0.1	[36]
5-methyl-2-thiozylmethacrylamide	Bulk	FAAS	26.6	9.1	14.8	82	0.9	[38]
2-thiozylmethacrylamide	Bulk	ICP-OES	304	93.2	79.4	76.3	0.4	This work

[a] 2-Vinylpyridine/5,6;14,15-dibenzo-1,4-dioxa-8,12-diazacyclopentadecane-5,14-diene.

Cu(II)–TMA complex possesses better selectivity over Co(II), Ni(II) and Zn(II) in comparison to the Cu(II)–MTMA and other ligands reported.

To examine the stability of the resin, a total of 10 loading and elution cycles were performed using the same column under the optimum conditions (e.g., pH, 5.5 and 1.0 mL of 2% (v/v) HNO_3 eluent). The IIP was found to be stable against treatment with mineral acids. No significant changes were observed in the retention performance of the column. Mean recovery was 98.2 ± 3.5% at 95% confidence level.

3.5. Figs. of merit and method validation

External calibration with aqueous multielement standards solutions of 0, 2, 5, 10, 15, 25 to 50 $\mu g\ L^{-1}$ was performed for determinations. The calibration standards were preconcentrated using the optimum conditions using the program in Table 2. Signals from five standard solutions (including blank) that bracket that of samples were used to calculate Cu(II) concentration in samples. The limit of detection (LOD) was calculated using standard solutions from 0 to 15 $\mu g\ L^{-1}$ (r^2 = 0.993–0.997). To determine LOD, a volume of 10 mL blank solution (n = 12) at pH 5.5 was passed through the column and eluted into 2 mL with 1 mL of 2% (v/v) HNO_3 followed by 1.0 mL of DI water. A limit of detection (3 s method) of 0.4 $\mu g\ L^{-1}$ was achieved, which was satisfactory for accurate determination of Cu(II) in natural water samples and other saline materials. The precision (%RSD) was 3.2% for preconcentration of 5.0 $\mu g\ L^{-1}$ Cu(II) standard solution.

The performance of the method was validated by analysis of fish otolith certified reference material (CRM 22) and bone ash (SRM 1400). The otolith sample contains trace elements in $CaCO_3$ matrix (38.8% Ca). The SRM 1400 is calcium phosphate, Ca (38.18%) and P (17.91%) along with Al, Fe, F, Mg, Sr and Zn as predominant matrix elements. The solutions of otolith and bone ash samples loaded onto the column contained about 1500 $\mu g\ mL^{-1}$ Ca(II) from dissolution of 0.05 g samples (see Section 2.6). The latter also contained about 2.2 $\mu g\ mL^{-1}$ Al(III), 2.8 $\mu g\ mL^{-1}$ Fe(III), and 0.75 $\mu g\ mL^{-1}$ Zn(II). The results for Cu(II) from these samples agreed with the indicative values (Table 7). This information is important as to show the ability of the resin to quantitatively extract Cu(II) from high Ca, Al, Fe, and Zn matrices. The samples were spiked with 1.0 or 10 $\mu g\ L^{-1}$ Cu(II) in determinations from coastal seawater and estuarine water. Mean recoveries for the spiked Cu(II)

were 91% for the coastal seawater and 96% for the estuarine water that did demonstrate that the Cu(II)–IIP would afford accurate determination of low levels of Cu(II) in seawater.

4. Conclusions

In this study, we have synthesized a new ion-imprinted polymer (IIP) incorporating 2-thiozylmethacrylamide (TMA) as chelating unit. In comparison with non-imprinted polymer, the IIP is highly selective toward Cu(II) over the common transition and heavy metal ions. Computational calculations also revealed that the stability of Cu(II)–TMA complex plays a critical role on the selectivity since imprinting on the surfaces is mediated during polymerization in the presence of the complex. In other words, the selectivity of the resulting material would likely be insufficient if the metal–ligand complex is not highly stable. Within this context, computational studies would be an important tool in predicting the viability of proposed ion-imprinted materials.

Determination of Cu(II) in saline samples by ICP-OES often demands separation and preconcentration of the element from the salt matrix. The Cu-IIP reported here possesses high capacity to achieve high enrichment factors; yet the procedure affords accurate measurement from various samples, such as seawater and fish otoliths samples, with relatively small enrichment factors (e.g., 5×). Further, the IIP is highly stable against treatments with mineral acids (e.g., 2% v/v HNO_3) and could be used for repetitive load/elute cycles without any significant deterioration in its retention performance. It should be noted that the IIP is uniquely suited for determination of Cu(II) in complex samples. Hence, the proposed method could also be adopted for cost-efficient determinations by FAAS, but at the cost of reduced enrichment factor or larger amount of sample since FAAS is more solution-demanding than ICP-OES.

Supplementary data to this article can be found online at http://dx.doi.org/10.1016/j.microc.2013.12.002.

Table 7
The results for Cu from the analysis of bone ash (SRM 1400) and fish otolith (CRM No: 22) certified reference materials, and coastal seawater and estuarine water samples. Values are given as mean ± standard deviation of five replicate analyses for each sample. Values in parenthesis are "information only". Spike concentrations are 1.0 and 10 $\mu g\ L^{-1}$ for coastal seawater and estuarine water samples, respectively.

Sample	Determined		Reported value	Recovery (%)
	Unspiked	Spiked		
Coastal seawater ($\mu g\ L^{-1}$)	1.22 ± 0.13	2.13 ± 0.21	–	91
Estuarine water ($\mu g\ L^{-1}$)	35.5 ± 0.7	45.1 ± 2.7	–	96
Bone ash (SRM 1400) ($\mu g\ g^{-1}$)	2.38 ± 0.14	–	(2.3)	103
Fish otolith (CRM 22) ($\mu g\ g^{-1}$)	0.72 ± 0.18	–	(0.74)	97

References

[1] L. Banci, I. Bertini, F. Cantini, S. Ciofi-Baffoni, Cellular copper distribution: a mechanistic systems biology approach, Cell. Mol. Life Sci. 67 (2010) 2563–2589.
[2] E.D. Harris, Copper, in: D.L. O'Dell, R.A. Sunde (Eds.), Handbook of nutritionally essential mineral elements, Markel Dekker, New York, 1997, pp. 231–273.

[3] M. Govindaraju, H.S. Shekar, The role copper in clinics of neurological disorder, Int. J. Res. Pharm. Chem. 1 (2011) 320–328.

[4] K.W. Bruland, J.R. Donat, D.A. Huchins, Interactive influences of bioactive trace metals on biological production in oceanic waters, Limnol. Oceanogr. 36 (1991) 1555–1577.

[5] F.M.M. Morel, N.M. Price, The biogeochemical cycles of trace metals in the oceans, Science 300 (2003) 944–947.

[6] A. Iwashita, T. Nakajima, H. Takanashi, A. Ohki, Y. Fujita, T. Yamashita, Determination of trace elements in coal and coal fly ash by joint-use of ICP-AES and atomic absorption spectrometry, Talanta 71 (2007) 251–257.

[7] J.C. Moss, C.J. Hardaway, J.C. Richert, J. Sneddon, Determination of cadmium copper, iron, nickel, lead and zinc in crawfish [*Procambrusclarkii*] by inductively coupled plasma optical emission spectrometry: a study over the 2009 season in Southwest Louisiana, Microchem. J. 95 (2010) 5–10.

[8] K. Pyrzynska, M. Trojanowicz, Functionalized cellulose sorbents for preconcentration of trace metals in environmental analysis, Crit. Rev. Anal. Chem. 29 (1999) 313.

[9] V. Camel, Solid phase extraction of trace elements, Spectrochim. Acta 58B (2003) 1177–1233.

[10] J. Haginaka, Selectivity of affinity media in solid-phase extraction of analytes, Trends Anal. Chem. 24 (2005) 407–415.

[11] B. Wen, X.-Q. Shan, Improved immobilization of 8-hydroxyquinoline on polyacrylonitrile fiber and application of the material to the determination of trace metals in seawater by inductively coupled plasma mass spectrometry, Anal. Bioanal. Chem. 374 (2002) 948–954.

[12] J. Otero-Romani, A. Moreda-Pineiro, P. Bermejo-Barrera, Trace metals distribution in surface and deep seawater from the Ría de Arousa estuary (north-western Spain). Study before and after the Prestige oil tanker sinking, Microchem. J. 97 (2011) 122–130.

[13] Z. Arslan, A.J. Paulson, Analysis of biogenic carbonates by inductively coupled plasma-mass spectrometry (ICP-MS). Flow injection on-line solid-phase preconcentration for trace element determination in fish otoliths, Anal. Bioanal. Chem. 372 (2002) 776–785.

[14] E. Vassileva, N. Furuta, Application of iminodiacetate chelating resin muromac A-1 in on-line preconcentration and inductively coupled plasma optical emission spectroscopy determination of trace elements in natural waters, Spectrochim. Acta Part B 58 (2003) 1541–1552.

[15] S.F.J. Vegueria, J.M. Godoy, R. Calixto de Campos, R.A. Gonçalves, Trace element determination in seawater by ICP-MS using online, offline and bath procedures of preconcentration and matrix elimination, Microchem. J. 106 (2013) 121–128.

[16] D. Kara, A. Fisher, S.J. Hill, Comparison of some newly synthesized chemically modified Amberlite XAD-4 resins for preconcentration and determination of trace elements by flow injection inductively coupled plasma-mass spectrometry (ICP-MS), Analyst 131 (2006) 1232–1240.

[17] V. Yilmaz, S. Kartal, Determination of some trace metals by FAAS after solid-phase extraction with amberlite XAD-1180/TAN chelating resin, Anal. Sci. 28 (2012) 515–521.

[18] I.S. Trujillo, E.V. Alonso, A.G. Torres, J.M.C. Pavón, Development of a solid phase extraction method for the multielement determination of trace metals in natural waters including sea-water by FI-ICP-MS, Microchem. J. 101 (2012) 87–94.

[19] J. Lee, E. Boyle, Y. Echegoyen-Sanz, J. Fitzsimmons, R. Zhang, R. Kayser, Analysis of trace metals (Cu, Cd, Pb, and Fe) in seawater using single batch nitrilotriacetate resin extraction and isotope dilution inductively coupled plasma mass spectrometry, Anal. Chim. Acta. 686 (2011) 93–101.

[20] D. Chen, B. Hu, M. He, C. Huang, Micro-column preconcentration/separation using thiacalix[4]arenetetracarboxylate derivative modified mesoporous TiO₂ as packing materials on-line coupled to inductively coupled plasma optical emission spectrometry for the determination of trace heavy metals in environmental water samples, Microchem. J. 95 (2010) 90–95.

[21] Y. Cui, X. Chang, Y. Zhai, X. Zhu, H. Zheng, N. Lian, ICP-AES determination of trace elements after preconcentrated with p-dimethylaminobenzaldehyde-modified nanometer SiO₂ from sample solution, Microchem. J. 83 (2006) 35–41.

[22] L. Zhang, Y. Zhai, X. Chang, Q. He, X. Huang, Z. Hu, Determination of trace metals in natural samples by ICP-OES after preconcentration on modified silica gel and on modified silica nanoparticles, Microchim. Acta 165 (2009) 319–327.

[23] S. Baytak, F. Zereen, Z. Arslan, Preconcentration of trace elements from water samples on a minicolumn of yeast (*Yamadazyma spartinae*) immobilized TiO₂ nanoparticles for determination by ICP-AES, Talanta 84 (2011) 319–323.

[24] L. Zhang, G. Cheng, C. Fu, Synthesis and characteristics of tyrosine imprinted beads via suspension polymerization, React. Funct. Polym. 56 (2003) 167–173.

[25] T.P. Rao, S. Daniel, J.M. Gladis, Tailored materials for preconcentration or separation of metals by ion-imprinted polymers for solid-phase extraction (IIP-SPE), Trends Anal. Chem. 23 (2004) 28–35.

[26] T. PrasadaRao, R. Kala, S. Daniel, Metal ion-imprinted polymers-novel materials for selective recognition of inorganics, Anal. Chim. Acta. 578 (2006) 105–116.

[27] E. Turiel, A.M. Esteban, Molecularly imprinted polymers for sample preparation: A review, Anal. Chim. Acta. 668 (2010) 87–99.

[28] A.N. Pustam, S.D. Alexadratos, Engineering selectivity into polymer-supported reagents for transition metal ion complex formation, React. Funct. Polym. 70 (2010) 545–554.

[29] E. Birlik, A. Ersöz, A. Denizli, R. Say, Preconcentration of copper using double-imprinted polymer via solid phase extraction, Anal. Chim. Acta. 565 (2006) 145–151.

[30] M. Shamsipur, J. Fasihi, A. Khanchi, R. Hassani, K. Alizadeh, H. Shamsipur, A stoichiometric imprinted chelating resin for selective recognition of copper(II) ions in aqueous media, Anal. Chim. Acta. 599 (2007) 294–301.

[31] S. Wang, R. Zhang, Selective solid-phase extraction of trace copper ions in aqueous solution with a Cu(II)-imprinted interpenetrating polymer network gel prepared by ionic imprinted polymer (IIP) technique, Microchim. Acta 154 (2006) 73–80.

[32] I. Dakova, I. Karadjova, I. Ivanov, V. Georgieva, B. Evtimova, G. Georgiev, Solid phase selective separation and preconcentration of Cu(II) by Cu(II)-imprinted polymethacrylicmicrobeads, Anal. Chim. Acta. 584 (2007) 196–203.

[33] A. Tobiasz, S. Walas, B. Trzewik, P. Grzybek, M.M. Zaitz, M. Gawin, H. Mrowiec, Cu(II)-imprinted styrene–divinylbenzene beads as a new sorbent for flow injection-flame atomic absorption determination of copper, Microchem. J. 93 (2009) 87–92.

[34] Y. Zhai, D. Yang, X. Chang, Y. Liu, Q. He, Selective enrichment of trace copper(II) from biological and natural water samples by SPE using ion-imprinted polymer, J. Sep. Sci. 31 (2008) 1195–1200.

[35] N.T. Hoai, D.K. Yoo, D. Kim, Batch and column separation characteristics of copper-imprinted porous polymer micro-beads synthesized by a direct imprinting method, J. Hazard. Mater. 173 (2010) 462–467.

[36] M. Shamsipur, A.B. Seidani, J. Fasihi, H. Sharghid, Synthesis and characterization of novel ion-imprinted polymeric nanoparticles for very fast and highly selective recognition of copper(II) ions, Talanta 83 (2010) 674–681.

[37] S. Walas, A. Tobiasz, M. Gawin, B. Trzewik, M. Strojny, H. Mrowiec, Application of a metal ion-imprinted polymer based on salen-Cu complex to flow injection preconcentration and FAAS determination of copper, Talanta 76 (2008) 96–101.

[38] V. Yılmaz, O. Hazer, Ş. Kartal, Synthesis, characterization and application of a novel ion-imprinted polymer for selective solid phase extraction of copper(II) ions from high salt matrices prior to its determination by FAAS, Talanta 116 (2013) 322–329.

[39] M. Andaç, R. Say, A. Denizli, Molecular recognition based cadmium removal from human plasma, J. Chromatogr. B 811 (2004) 119–126.

[40] G.Z. Fang, J. Tan, X.P. Yan, An ion-imprinted functionalized silica gel sorbent prepared by a surface imprinting technique combined with a sol–gel process for selective solid-phase extraction of cadmium(II), Anal. Chem. 77 (2005) 1734–1739.

[41] A. Ersöz, R. Say, A. Denizli, Ni(II) ion-imprinted solid-phase extraction and preconcentration in aqueous solutions by packed-bed columns, Anal. Chim. Acta. 502 (2004) 91–97.

[42] J. Otero-Romaní, A. Moreda-Piñeiro, P. Bermejo-Barrera, A. Martin-Esteban, Ionic imprinted polymer for nickel recognition by using the bi-functionalized 5-vinyl-8-hydroxyquinoline as a monomer: Application as a new solid phase extraction support, Microchem. J. 93 (2009) 225–231.

[43] J. Otero-Romaní, A. Moreda-Piñeiro, P. Bermejo-Barrera, A. Martin-Esteban, Inductively coupled plasma–optical emission spectrometry/mass spectrometry for the determination of Cu, Ni, Pb and Zn in seawater after ionic imprinted polymer based solid phase extraction, Talanta 79 (2009) 723–729.

[44] J. Zhao, B. Han, Y. Zhang, D. Wang, Synthesis of Zn(II) ion-imprinted solid-phase extraction material and its analytical application, Anal. Chim. Acta. 603 (2007) 87–92.

[45] X. Zhu, Y. Cui, X. Chang, X. Zou, Z. Li, Selective solid-phase extraction of lead(II) from biological and natural water samples using surface-grafted lead(II)-imprinted polymers, Microchim. Acta 164 (2009) 125–132.

[46] Ö. Saatçilar, N. Satiroglu, R. Say, S. Bektas, A. Denizli, Binding behavior of Fe(III) ions on ion-imprinted polymeric beads for analytical applications, J. Appl. Polymer Sci. 101 (2006) 3520–3528.

[47] E. Birlik, A. Ersöz, E. Acikkalp, A. Denizli, R. Say, Cr(III)-imprinted polymeric beads: Sorption and preconcentration studies, J. Hazard. Mater. 140 (2007) 110–116.

[48] Y. Liu, X. Chang, D. Yang, Y. Guo, S. Meng, Highly selective determination of inorganic mercury(II) after preconcentration with Hg(II)-imprinted diazoaminobenzene–vinylpyridine copolymers, Anal. Chim. Acta. 538 (2005) 85–91.

[49] Z. Fan, Hg(II)-imprinted thiol-functionalized mesoporous sorbent micro-column preconcentration of trace mercury and determination by inductively coupled plasma optical emission spectrometry, Talanta 70 (2006) 1164–1169.

[50] F. Zereen, V. Yilmaz, Z. Arslan, Multielement solid phase preconcentration using a chelating resin of styrene divinylbenzene copolymer and application to analysis of seawater and fish otoliths by inductively coupled plasma mass spectrometry (ICP-MS), Anal. Lett. (2013), http://dx.doi.org/10.1080/00032719.2013.831428 (09 Sep).

[51] R.D. Shannon, Revised effective ionic radii and systematic studies of interatomic distances in halides and chalcogenides, Acta Crystallogr. 32 (1976) 751–767.